Platelet factor 4 induces bone loss by inhibiting the integrin α5-FAK-ERK pathway

Hao Liu
Peking University School and Hospital of Stomatology & National
Qiwei Zhang
Chinese Academy of Medical Sciences
Ranli Gu
Peking University School and Hospital of Stomatology & National
Wei Li
Peking University School and Hospital of Stomatology & National
Yunsong Liu
Peking University School and Hospital of Stomatology & National
Yongsheng Zhou (kqzhouysh@hsc.pku.edu.cn)
Peking University School and Hospital of Stomatology & National

Research Article

Keywords:

Posted Date: September 9th, 2022

DOI: https://doi.org/10.21203/rs.3.rs-2028573/v1

Abstract

Background

The effect of platelet factor 4 (PF4) on bone marrow mesenchymal stem cells (BMMSCs) and osteoporosis remains poorly understood. Hence, this study aimed to evaluate the effects of PF4-triggered bone destruction of mice and determine the underlying mechanism.

Methods

Firstly, in *vitro* cell proliferation and cell cycle of BMMSCs were assessed by a CCK8 assay and flow cytometry, respectively. Osteogenic differentiation was confirmed using staining and quantification of alkaline phosphatase and alizarin red. Next, an osteoporotic mouse model was established by performing bilateral ovariectomy. Furthermore, the Pf4 concentrations were obtained using ELISA. The bone microarchitecture of the femur was evaluated by microCT and histological analyses. Finally, the key regulators on osteogenesis and pathways were investigated by *q*PCR and WB.

Results

Human PF4 widely and moderately lessened the cell proliferation and osteogenic differentiation ability of BMMSCs. Furthermore, the level of Pf4 in the serum and BM were generally increased, whereas the bone microarchitecture deteriorated due to OVX surgery. Moreover, *in vivo* mouse Pf4 supplementation triggered bone deterioration of the femur. Besides, several key regulators of osteogenesis were down-regulated and the integrin α5 (ITGA5)-FAK-ERK pathway was inhibited due to PF4 supplementation.

Conclusions

PF4 may be related to OVX-induced bone loss triggered by the suppression of bone formation *in vivo* and alleviated BMMSC osteogenic differentiation through inhibiting the ITGA5-FAK-ERK pathway.

1. Introduction

Osteoporosis is a chronic syndrome characterized by a loss of bone mass and destruction of the bone microarchitecture, which finally leads to excessive skeletal fragility [1]. Mechanistically, osteoporosis occurs due to an imbalance between osteoblast-mediated bone formation and bone resorption by osteoclasts (i.e., higher levels of bone resorption than bone formation) [2]. Current strategies of osteoporotic prevention and treatment focus on promoting bone regeneration, suppressing bone resorption, or a combination of both [3]. Recently, some targeted drugs for osteoporosis have been approved for clinical use and exhibit excellent curative effects [4–6].

As a predominant source of osteoblasts, it is crucial to maintain osteogenic differentiation and proliferation of bone marrow mesenchymal stem cells (BMMSCs) to preserve bone homeostasis [7]. Furthermore, several evidences have revealed that BMMSC-mediated osteogenic differentiation and proliferation can be downregulated or impaired by multiple factors in the bone marrow (BM), which is markedly associated with osteoporosis [8–10].

It has been well established that the osteogenic differentiation and proliferation of BMMSCs is suppressed by several cytokines [11–13]; however, the relationship between some cytokines and BMMSCs is unclear. Platelet factor 4 (PF4), also termed C-X-C motif ligand 4 or CXCL4, is a 7.8 kDa platelet alpha-granule protein synthesized by megakaryocytes in the BM and belongs to the CXC chemokine subfamily [14]. In general, PF4 plays multiple roles in modulating hematopoiesis, angiogenesis, cell proliferation [15–20]. Recent research has demonstrated that PF4 secretion by megakaryocytes can directly regulate hemopoietic stem cell (HSC) quiescence in the local HSC niche of the BM. Similarly, the percentage of HSCs was lower following treatment with PF4 compared with those treated with PBS [21]. However, the specific role of PF4 in BMMSCs has never been elucidated. Given the multiple physiological effects of PF4, we speculated that it may downregulate the proliferation or osteogenic differentiation of BMMSCs, which may be relevant to osteoporosis.

Recently, several studies have elucidated that platelet factors regulate the function of recipient cells by integrins, which belong to the family of transmembrane adhesion receptors formed by the 19 α and 8 β subunits [22–24]. These subunits can interact to form 24 heterodimeric receptors via noncovalent binding, which exist in the recipient cell surface to recognize and respond to various proteins, such as PF4, platelet factor XIII, or osteopontin [25]. Accordingly, integrins have functions in regulating cellular proliferation, migration, and differentiation [26]. Moreover, integrin signaling can be transduced into the cytoplasm by the intracellular signaling molecule, like focal adhesion kinase (FAK), which can directly bind to focal adhesion sites located in the cytoplasmic domain of integrins. Besides, several downstream molecules also are involved in integrin-FAK pathway, such as extracellular signal-regulated kinase (ERK), which can directly inhibit caspase 9 activation by phosphorylation of Thr^{125} located in conserved mitogen activated protein kinase (MAPK) consensus site [27].

Hence, this study aimed to confirm the relationship between PF4 and osteoporosis, evaluate the effects of PF4-triggered bone destruction in mice *in vivo*, and determine the mechanism underlying the suppression of osteogenesis or proliferation of BMMSCs induced by PF4.

2. Materials And Methods

2.1. Cell proliferation and migration assays. To explore the effects of PF4 on BMMSC proliferation and migration, CCK8 and transwell assays were performed, respectively [28, 29]. Briefly, human BMMSCs (#7504, Science Cell Research Laboratories, CA, USA) were cultivated in maintenance medium [DMEM containing 10% fetal bovine serum (FBS), 100 U/mL penicillin G, and 100 mg/mL streptomycin] at 37°C in an atmosphere of 5% CO_2. BMMSCs of passage 3–5 were co-cultured with PBS, 0.2 μg/mL

recombinant human PF4 (hPF4, #SRP3142, Sigma-Aldrich, Saint Louis, MO, USA), 1 μg/mL hPF4, and 1 μg/mL hPF4 + 30 μg/mL Heparin (hPF4 antagonist) (#H3149, Sigma-Aldrich, Saint Louis, MO, USA). CCK8 (#CK04, Dojindo Laboratories, Kumamoto, Japan) and transwell assays (#3472, Corning, Corning, NY, USA) were detected according to the manufacturer's SOPs. All cell-based experiments were repeated at least three times.

2.2. Flow cytometry. To investigate the effects of PF4 on the cell cycle, BMMSCs treated as mentioned above were measured by flow cytometry (FCM) [30]. Briefly, the BMMSCs were harvested and resuspended in PBS and fixed using cold alcohol. Subsequently, the PI/RNase staining buffer (#550825, Becton, Dickinson and Company, NJ, USA) was added to the BMMSCs and incubated. Finally, the cell cycle was tested using a BD LSRII flow cytometer (Becton, Dickinson and Company, NJ, USA).

2.3. Staining and quantification of alkaline phosphatase and alizarin red. To investigate the osteogenic effect of PF4 on BMMSCs, the staining and quantification of alkaline phosphatase (ALP) and alizarin red were undertaken [31]. hBMMSCs were seeded at 40,000 cells/well in 6-well plates and cultured in osteogenic medium [fresh DMEM containing 10 nM dexamethasone (#D4902, Sigma-Aldrich, Saint Louis, MO, USA), 10mM β-glycerophosphate (#G9422, Sigma-Aldrich, Saint Louis, MO, USA), 0.2mM L-ascorbic acid (#A4403, Sigma-Aldrich, Saint Louis, MO, USA), 10% (v/v) FBS, and penicillin/streptomycin]. And hBMMSCs were first stained with a NBT/BCIP staining kit (CoWin Biotech, Beijing, China) after culturing for one week for ALP and a 2% alizarin red S (ARS) staining solution (Sigma-Aldrich, Saint Louis, MO, USA) after culturing for three weeks for alizarin red, respectively.

For ALP quantification, the total protein of the BMMSCs was detected by a BCA protein assay kit (Thermo Scientific, Waltham, MA, USA) according to the manufacturer's SOP. Subsequently, the ALP activity was measured using an ALP assay kit (Nanjing Jiancheng Bioengineering Institute, Nanjing, China) and standardized to the total protein. Alizarin red quantification was achieved by ARS staining of the BMMSCs and was solubilized by cetylpyridinium chloride. The OD value of the dissolved ARS was tested spectrophotometrically.

2.4. Animal and administration procedures. Eight-week-old female C57BL6/J mice (Vital River Inc., Beijing, China) were housed in the SPF room according to the "Guide for the Care and Use of Laboratory Animals". All animal experiments were approved by the Animal Care and Use Committee of Peking University Health Science Center (approval number: LA2019019; Beijing, China). First, to explore the relationship between PF4 and osteoporosis, a classic osteoporotic animal model was established via ligaturing bilateral ovariectomy (OVX). Generally, 60 mice were split into 10 groups of 6 mice, and the ligation of bilateral OVX was undertaken using standard methods [32]. After surgery, euthanasia was performed on each group every two weeks (at least) until week 12. The serum and BM of tibia were obtained to detect the concentration of Pf4 using ELISA or the relative expression of *Pf4* using *q*PCR. To obtain BM from the tibia, the tibia were dissected free from soft tissue thoroughly and the tip of the tibia was removed with a rongeur. Next, the BM was flushed with maintenance medium [Dulbecco's modified Eagle's medium (high glucose) (DMEM, #C11995500BT) containing 10% fetal bovine serum (FBS,

#16000-044), 100 U/mL penicillin G, and 100 mg/mL streptomycin (#15140-122)] (GIBCO, Life technologies, Invitrogen, NY, USA) (for ELISA) or TRIzol (for *q*PCR) (#15596018, Life technologies, Invitrogen, NY, USA) by inserting a syringe needle into one end of the bone under aseptic conditions. Besides, the femurs were dissected for microCT and histology. To investigate the effects on Pf4-induced bone loss, 30 mice were split into three groups comprised of 10 mice and treated with PBS, 2 μg recombinant mouse Pf4 (mPf4), and 5 μg mPf4 (i.p., dissolved in NS, every other day) (#SRP6229, Sigma-Aldrich, Saint Louis, MO, USA). The mice were euthanized on week 8 after the injection. Tissues were obtained using the methods as described above.

2.5. MicroCT analysis. To evaluate the differences in bone morphometry in these groups, a microCT was performed using an Inveon MM system (Siemens, Munich, Germany) [33]. Briefly, the images of the femurs were obtained using the following parameters: pixel size of 9.21 μm; current of 220 μA; voltage of 60 kV; and exposure time of 1500 ms. The bone mineral density (BMD) and bone morphometric parameters were analyzed using Inveon Research Workplace software (Siemens).

2.6. Histological analysis. To further confirm PF4-induced bone loss, the femurs were decalcified using a 10% EDTA solution after fixation in formalin. The 5-μm slicing was obtained using standard procedures and stained with H&E.

To investigate the histomorphometric changes in the bone dynamics, the undecalcified bone slicing and following analyses were performed [34]. Briefly, on the 10th and 3rd day prior to euthanasia, the mice were intraperitoneally injected with alizarin-3-methyliminodiacetic acid (30 mg/kg, #A3882, Sigma-Aldrich, Saint Louis, MO, USA) and calcein (10 mg/kg, #C0875, Sigma-Aldrich, Saint Louis, MO, USA), respectively. The femurs were ground up and polished into approximately 50-μm slices using standard procedures using the EXAKT precision cutting and grinding system (EXAKT Apparatebau, Hamburg, Germany). Subsequently, dynamic histomorphometric parameters were analyzed using Bioquant software (BioQuant, San Diego, CA, USA).

2.7. ELISA. An enzyme-linked immunosorbent assay (ELISA) was used to test the concentration of Pf4 in the serum and BM from tibia. In brief, the serum was separated from the blood and BM supernatants were flushed out using PBS. A Pf4 ELISA kit (#MCX400, R&D systems, Minnesota, USA) was used to detect the concentration of Pf4 in the serum and BM according to the manufacturer's SOPs. At a minimum, the samples were tested in duplicate.

2.8. RNA extraction and qPCR. The total RNA of BMMSCs treated with different factors was extracted using an RNeasy Mini Kit (#74104, Qiagen, Cary, NC, USA). The cDNA was synthesized with a PrimeScript RT Reagent Kit (#RR037A, Takara, Tokyo, Japan). *q*PCR was performed using the 7500 Real-Time PCR Detection System (Applied Biosystems, CA, USA). The primers are listed in Table 1 and the procedure was performed as follows: 95°C for 10 min, followed by 40 cycles of 95°C for 15 s, and 60°C for 1 min. Finally, the data were analyzed with the $2^{-\Delta CT}$ method through *GAPDH/Gapdh* for normalization [35].

Table 1
Sequences of the primers used for qPCR.

	Forward primer (5' to 3')	Reverse primer (5'-3')
GAPDH	CGGACCAATACGACCAAATCCG	AGCCACATCGCTCAGACACC
PF4	TGGAGGTGATCAAGGCGGGAC	GGCAGCTTCTACCTAACTCTCCA
RUNX2	ACTACCAGCCACCGAGACCA	TGGCAGGTACGTGTGGTAGT
SP7	CCTCCTCAGCTCACCTTCTC	GTTGGGAGCCCAAATAGAAA
SPP1	ATGATGGCCGAGGTGATAGT	ACCATTCAACTCCTCGCTTT
SPARC	AGTGCACCCTGGAGGGCACC	TGCTTGATGCCGAAGCAGCC
COL1A1	GAGGGCCAAGACGAAGACATC	CAGATCACGTCATCGCACAAC
ITGA5	TTCGCCTCTGGGAGGTTTAG	TCCGCGTCTAAGTTGAAGCC
CCND1	GGATGCTGGAGGTCTGCGA	AGAGGCCACGAACATGCAAG
CDK4	AGTTCGTGAGGTGGCTTTA	GGGTGCCTTGTCCAGATA
CDKN1B	ATGTCAAACGTGCGAGTGTC	TCTGTAGTAGAACTCGGGCAA
Gapdh	TGCACCACCAACTGCTTAGC	GGCATGGACTGTGGTCATGAG
Pf4	TGGAGGTGATCAAGGCTGGAC	GGCAGCTCTTAGCTAACTCTCCA

GAPDH/Gapdh, glyceraldehyde-3-phosphate dehydrogenase; *PF4/Pf4*, platelet factor 4; *RUNX2*, RUNX family transcription factor 2; *SP7*, Sp7 transcription factor; *SPP1*, secreted phosphoprotein 1; *SPARC*, secreted protein acidic and cysteine rich; *COL1A1*, collagen type I alpha 1 chain; *ITGA5*, integrin subunit alpha 5; *CCND1*, cyclin D1; CDK4, cyclin dependent kinase 4; CDKN1B, cyclin dependent kinase inhibitor 1B.

2.9. Construction of ITGA5i and ITGA5 shRNA lentivirus. The silence/overexpression of ITGA5 were performed using ITGA5-targeting (ITGA5i) oligonucleotide sequence or ITGA5 overexpression lentivirus designed by GeneChem (Shanghai, China) as previously described [36]. Briefly, the ITGA5i oligonucleotide sequence was CTCCTATATGTGACCAGAGTT and ITGA5 overexpression lentivirus contained only and full transcript of ITGA5 gene. Besides, the lentiviral work vector is Ubi-MCS-3FLAG-SV40-EGFP-IRES-puromycin. The BMMSCs were infected with the above-mentioned lentivirus at a multiplicity of infection of 20.

2.10. Western blotting. Western blotting (WB) was performed using the standard procedure as previously described [37]. Briefly, the cells were lysed to obtain total protein using a radioimmunoprecipitation assay (RIPA) buffer mixed protease inhibitor (#R0010, Solarbio, Beijing, China). After that, the lysates were centrifuged at 12000 rpm, 30 min in 4 °C. The total protein concentrations were detected by Pierce BCA

protein assay kit (#23225, Thermo Scientific, Waltham, MA, USA). The 20 μg protein extracts were separated by 10% SDS PAGE and transferred onto polyvinylidene difluoride (PVDF) membrane (#C3117, Merck Millipore, Darmstadt, Germany). And then, the membranes were incubated at 4 °C overnight with respective primary antibodies (Abcam, UK), including CCND1 (#ab40754, EP272Y, 1:2000), CDK4 (#ab108357, EPR4513-32-7, 1:1000), CDKN1B (#ab32034, Y236, 1:5000), SP7 (#ab209484, EPR21034, 1:1000), SPP1 (#ab214050, EPR21139-316, 1:1000), SPARC (#ab207743, EPR20121, 1:1000), RUNX2 (#ab236639, EPR22858-106, 1:1000), COL1A1 (#ab138492, EPR7785, 1:1000), ITGA2 (#ab181548, EPR17338, 1:5000), ITGA5 (#ab150361, EPR7854, 1:10000), ITGA6 (#ab181551, EPR18124, 1:2000), ITGB1 (#ab52971, Integrin beta 1, EP1041Y, 1:10000), ITGB3 (#ab119992, EPR2342, 1:1000), ITGB4 (#ab133682, EPR8559, 1:1000), FAK (#ab40794, EP695Y, 1:2000), p-FAK (#ab81298, phosphor Y397, EP2160Y, 1:1000), ERK 1/2 (#ab184699, ERK1+ERK2, EPR17526, 1:10000), p-ERK 1/2 (#ab201015, ERK1 (phospho T202)+ERK2 (phosphor T185), EPR19401, 1:1000), and GAPDH (#ab181602, EPR16891, 1:10000) following by detection on immunoreactive protein bands after incubation for 1 h by ECL kit (#CW0049M, CWBIO, Beijing, China) with horseradish peroxidase-linked anti-rabbit secondary antibodies (#ab7090, 1:5000, Abcam, UK) at room temperature.

2.11. Statistical analysis. Statistical analysis was conducted using IBM SPSS Statistics 20.0 software (SPSS, Chicago, IL, USA). An independent two-tailed Student's *t*-test or one-way analysis of variance (ANOVA) with a post hoc analysis of the least significant difference (LSD) was applied. Data were expressed as the mean ± standard deviation (SD). A threshold P value < 0.05 was considered statistically significant.

3. Results

3.1. PF4 decreases the cell proliferation and migration ability of BMMSCs. To explore the effects on BMMSCs of PF4, the detection of cell proliferation or migration of BMMSCs was initially performed. The CCK8 assay indicated that the cell proliferation rate of the BMMSCs in the 0.2 μg/mL PF4 and 1 μg/mL PF4 groups was lower than those in the 0 μg/mL PF4 and PF4 + Heparin groups from day 3 to day 6 (Fig. 1a). Furthermore, the cell cycle detected by FCM showed that the BMMSCs in the 0.2 μg/mL PF4 and 1 μg/mL PF4 groups had a markedly decreased proportion of cells in S phase compared to those in the CTL group. In addition, the cell proportion in S phase in the 1 μg/mL PF4 group also exhibited a significant decline compared to the PF4 + Heparin group. Accordingly, the cell counts in the G_0/G_1 and/or G_2/M phase of the 0.2 μg/mL PF4 and 1 μg/mL PF4 groups were dramatically increased compared with those in the CTL and PF4 + Heparin groups (Fig. 1b and c). Moreover, the relative expression of *CCND1* and *CDK4* in BMMSCs in the 0.2 μg/mL PF4 and 1 μg/mL PF4 groups were significantly decreased compared with those in the CTL group. Furthermore, the PF4 + Heparin group exhibited a significant increase in the relative expression of *CCND1* compared with those in the 0.2 μg/mL PF4 and 1 μg/mL PF4 groups, and markedly decreased relative expression of *CCND1* compared to the CTL group. In contrast, the relative expression of *CDKN1B* in the 0.2 μg/mL PF4 and 1 μg/mL PF4 groups was higher than that in the CTL and PF4 + Heparin groups. Moreover, the 1 μg/mL PF4 group was associated with a

dramatic increase in the relative expression of *CDKN1B* compared to the 0.2 μg/mL PF4 group. Furthermore, the PF4 + Heparin group also exhibited a significant increase in the relative expression of *CDKN1B* compared with the CTL group. Moreover, the tendencies of protein expression levels of CCND1, CDK4, and CDKN1B were similar to the mRNA expression levels of the above-mentioned markers (Fig. 1d).

Besides, a transwell assay demonstrated that the cell migration ability of BMMSCs in the 0.2 μg/mL PF4 and 1 μg/mL PF4 groups was lower than that of the CTL and PF4 + Heparin groups (Fig. 1e and f).

3.2. PF4 attenuates the ability of osteogenic differentiation of BMMSC. For the staining and quantification of ALP, the 0.2 μg/mL PF4 and 1 μg/mL PF4 groups exhibited dramatically decreased ALP activity compared with those of the osteogenic medium (OM) and PF4 + Heparin groups. Furthermore, the PF4 + Heparin group exhibited a significant increase in ALP activity compared with that of the CTL group and markedly decreased ALP activity compared to that of the OM group. Moreover, the ALP activity of the OM and 0.2 μg/mL PF4 group was higher than that of the CTL group (Fig. 2a and b).

For the staining and quantification of ARS, the absorbance of the ARS solution dissolved in calcium nodules in the 0.2 μg/mL PF4 and 1 μg/mL PF4 groups was lower than those in the OM and PF4 + Heparin groups, and higher than that in the CTL group, which was consistent with the ALP quantification results. Moreover, the 1 μg/mL PF4 group showed a dramatic decrease in the absorbance of the ARS solution compared with that of the 0.2 μg/mL PF4 group ($p < 0.05$). Moreover, the OM and PF4 + Heparin groups exhibited a significant increase in the absorbance of the ARS solution compared with that of the CTL group (Fig. 2c).

3.3. Trends of PF4 concentration in BM and serum post-OVX surgery. To explore the relationship between the levels of Pf4 and OVX-triggered bone destruction, the variation tendency of Pf4 levels in serum and BM was investigated in OVX and Sham mice. In general, the level of Pf4 was increased in OVX mice compared with that of Sham group, whereas the bone mass and microarchitecture were deteriorated due to OVX surgery. In detail, the concentrations of serum Pf4 demonstrated a significant increase after OVX surgery, only interrupted by a temporary through/dip at around 6–8 weeks ($p < 0.05$, respectively) (Fig. 3a). Consistent with serum Pf4, the concentrations of Pf4 in the BM also had a significant increase from 2 weeks, only interrupted by a temporary through/dip at around 4 weeks ($p < 0.05$, respectively) (Fig. 3b). Moreover, the variation tendency of the relative expression of *Pf4* in the BM was analogous to the Pf4 concentration in the BM and exhibited a more robust change (Fig. 3c). As expected, the femur of OVX mice exhibited a severe bone loss at 6 and 12 weeks compared with that of Sham mice (Fig. 3d, Figure S1).

3.4. Supplementation of Pf4 triggers bone destruction. To further investigate the effects on Pf4-triggered bone destruction, the BMD and bone microarchitecture were evaluated. In short, the BMD and bone microarchitecture of the femur decreased along with the increasing dose of mPf4 injection. Specifically, the 2 μg Pf4 and 5 μg Pf4 groups exhibited a significant decrease in the Ma. BMD, bone volume/total volume (BV/TV), trabecular thickness (Tb.Th), and trabecular number (Tb.N), as well as a substantial

decrease in the bone surface area/bone volume (BS/BV) compared with those in the CTL group. Moreover, the 5 μg Pf4 group exhibited a lower Ma.BMD compared to that that in the 2 μg Pf4 group, as well as a higher trabecular separation (Tb.Sp) than in the CTL group (Fig. 4a and b). As expected, the levels of Pf4 in the serum and BM in the 2 μg Pf4 and 5 μg Pf4 groups were significantly increased compared to the CTL group. Additionally, the concentrations of Pf4 in the serum and BM in the 5 μg Pf4 group exhibited significant increases compared to that in the 2 μg Pf4 group (Fig. 4c).

Besides, there was a dramatic decline in the mineral apposition rate (MAR) and bone formation rate/bone surface (BFR/BS) of the 2 μg Pf4 and 5 μg Pf4 groups compared to that of the CTL group (Fig. 5).

3.5. PF4 inhibits the ITGA5-FAK-ERK pathway to reduce the osteogenic differentiation of BMMSCs. Next, to investigate the underlying mechanisms of PF4-mediated regulation of osteogenic differentiation of BMMSCs, some key regulators of osteogenesis were screened by *q*PCR. Specifically, the 0.2 μg/mL PF4 and 1 μg/mL PF4 groups exhibited a significant decrease in the relative expression of *RUNX2*, *SP7*, *SPP1*, *SPARC*, and *COL1A1* compared with that in the OM and PF4 + Heparin groups. Moreover, the relative expression of the four above-mentioned osteogenic genes (except for *SP7*) in the 1 μg/mL PF4 group was lower than those in the 0.2 μg/mL PF4 group. Moreover, the tendency of protein expression levels of 5 osteogenic markers were similar to the mRNA expression levels of the above-mentioned genes (Fig. 6a).

In addition, to explore the pathway mediated by PF4 under the condition of osteogenic differentiation of BMMSCs, 6 typical integrin subunits were screened using WB. Of note, the protein expression level of integrin α5 (ITGA5), rather than the other 5 typical integrin subunits, was suppressed by PF4 in a dose-dependent manner. Moreover, similar to the above-mentioned osteogenic genes, the relative *integrin α5* (*ITGA5)* expression in the 0.2 μg/mL PF4 and 1 μg/mL PF4 groups was lower than those in the OM and PF4 + Heparin groups (Fig. 6b).

Furthermore, ITGA5 protein expression decreased in ITGA5i-LV group and increased in ITGA5-LV group, which was similar to the protein expression of p-FAK, p-ERK1/2, and ALP (Fig. 6c and d).

4. Discussion

This study revealed that PF4 widely lessened the cell proliferation, cell cycle, cell migration, and osteogenic differentiation of BMMSCs. Accordingly, research into the molecular mechanisms of osteogenesis validated the downregulation of several key regulators of osteogenesis and that the ITGA5-FAK-ERK pathway was inhibited due to PF4 supplementation. Further investigation demonstrated that the level of Pf4 in the serum and BM were generally increased, whereas the bone mass and microarchitecture were deteriorated in mice as a result of OVX surgery. Furthermore, *in vivo* supplementation of mPf4 triggered bone loss in mice due to the suppression of bone formation (Fig. 7).

In the present study, the proliferation and cell cycle of the BMMSCs were suppressed by PF4. Previous studies also validated the ability of PF4 to maintain the cell quiescence of HSCs to regulate the survival and self-renewal of HSCs [21, 38], which was consistent with our results. It is important to note that it was

moderate and reversible to suppress the cell proliferation and cell cycle of BMMSCs in order to cell survival and self-renewal rather than cell death. Hence, according to *vivo* and *vitro* results, we speculated that at first, BMMSCs rapidly underwent proliferation and osteogenic differentiation to avoid quick bone loss after OVX surgery. However, PF4 maintained the BMMSC population and pluripotency to prevent BMMSC excessive exhaustion. Finally, the balance was broken out and OVX-induced bone loss happened because of PF4 in a consistent high levels, which may indicate that it is more important to maintain the BMMSC population and pluripotency for the entire body in comparison with rescuing bone loss. The rule on BMMSC regulation requires further investigation.

Our previous study revealed that aspirin prompted *in vitro* cell migration and *in vivo* cell homing of adipose-derived stromal cells (ASCs) [39]; however, the associated mechanisms remain unknown. Interestingly, this study revealed that the cell migration of BMMSCs was suppressed by PF4 in a dose-dependent manner. Of note, recent research has supported the hypothesis that the systemic administration of aspirin induced a significant decrease in the level of PF4 in a rat model of periodontal disease [40, 41]. Taken together, these studies suggested that aspirin promoted the cellular migration of stem cells due to the inhibition of PF4 levels.

In addition, the results demonstrated that PF4 attenuated the osteogenic differentiation of BMMSCs; however, Chen *et al.* showed that ALP staining of the PF4 group was weaker than that of the CTL group, which was similar to the results of our study [42]. Further research uncovered that PF4 downregulated five key regulators of osteogenesis and inhibited the ITGA5-FAK-ERK pathway to descend the osteogenic differentiation of BMMSCs. Aidoudi *et al.* deemed that PF4 could interact with the integrins, αvβ3/αvβ5/α5β1, to suppress endothelial cell adhesion and migration and further contribute to its antiangiogenic effect [24]. Moreover, the study by Kulkarni *et al.* revealed that platelet factor XIII limited platelet aggregate formation and thrombus growth by regulating the integrin, αIIbβ3 [22]. In addition, Lishko *et al.* also demonstrated that leukocyte integrin Mac-1 functions as a functional receptor of PF4 [23]. In this study, we also found that PF4 could regulate ITGA5 to attenuate osteogenic differentiation, which is consistent with the findings of the above studies. It is important to note that recent research has validated that the integrin-FAK-ERK pathway plays a vital role in bone metabolism. For example, the findings of Viale-Bouroncle *et al.* found that Laminin regulated the osteogenic differentiation of dental follicle cells by the integrin α2β1-FAK-ERK pathway [43]. Moreover, Chandran *et al.* showed that the biocomposite scaffold containing the phytomolecule diosmin could promote osteoblast differentiation and bone regeneration in mouse BMMSCs through the integrin-FAK-ERK pathway [44]. In addition, Chen *et al.* reported that osteopontin increased the migration of chondrosarcoma cells through the integrin αvβ3, FAK, and ERK pathways [45]. Furthermore, another study found that OPN promoted MSC migration via the integrin β1, FAK, and ERK pathways [46].

In this study, we first found that the level of Pf4 generally increased in OVX mice compared with Sham mice. Of note, the levels of Pf4 fluctuated twice prior to euthanasia rather than a consistent increase. Specifically, the concentration of Pf4 in the BM raised quickly since OVX surgery and reached the peak at the third week. However, the Pf4 level declined quickly on the fourth week and slowly raised again

between the sixth and tenth week. Surprisingly, the levels of Pf4 began to decline at 12 weeks. As expectedly, the variation tendency of the Pf4 level in the serum was similar to that in BM. Considering that PF4 was stored in platelet alpha granule and can be quickly released to serum or BM [14], we speculated that the first peak of Pf4 was from platelets. Following PF4 in the platelet was exhausted, the PF4 was synthesized by megakaryocytes and gradually released to serum or BM [21]. Hence, Pf4 level raised again and maintained a higher level in OVX mice compared to Sham group. Furthermore, we found that supplementing Pf4 triggered the decreased BMD and deterioration of bone microarchitecture, which means that Pf4 indeed played a key role in bone loss.

There are some limitations of this study. *In* v*ivo* mechanisms of the increased PF4-triggered bone loss should be explored to confirm the cause-and-effect relationship of PF4 and bone.

5. Conclusions

PF4 widely lessened the cell proliferation and osteogenic differentiation of BMMSCs by inhibiting ITGA5-FAK-ERK pathway. Furthermore, Pf4 triggered bone loss in mice due to the suppression of bone formation.

Declarations

Data Availability

The data used to support the findings of this study are available from the corresponding author upon request.

Conflicts of Interest

The authors declare that they have no conflicts of interest.

Funding Statement

This work was supported by grants from the National Natural Science Foundation of China [grant numbers 81700935, 81970908, and 81870742], and the grant from the Beijing Natural Science Foundation [L182006], and CAMS Innovation Fund for Medical Sciences [2019-I2M-5-038].

Authors' Contributions

Y.Z. and Y.L. conceived and supervised the study; H.L. designed the experiments; H.L., Q.Z., R.G., and W.L. performed the experiments; H.L. analyzed the data; H.L. and Q.Z. wrote the manuscript; Y.Z. and Y.L. revised the manuscript. Hao Liu and Qiwei Zhang contributed equally to this study.

References

1. J. M. Lane, L. Russell, and S. N. Khan, "Osteoporosis," Clinical Orthopaedics and Related Research, vol. 372, pp. 139–150, 2000.
2. M. Srivastava, and C. Deal, "Osteoporosis in elderly: prevention and treatment," Clinics in Geriatric Medicine, vol. 18, no. 3, pp. 529–555, 2002.
3. I. R. Reid, "A broader strategy for osteoporosis interventions," Nature Reviews: Endocrinology, vol. 16, no. 6, pp. 333–339, 2020.
4. E. D. Deeks, "Denosumab: A Review in Postmenopausal Osteoporosis," Drugs and Aging, vol. 35, no. 2, pp. 163–173, 2018.
5. A. Tominaga, K. Wada, Y. Kato, et al., "Early clinical effects, safety, and appropriate selection of bone markers in romosozumab treatment for osteoporosis patients: a 6-month study," Osteoporosis International, vol. 32, no. 4, pp. 653–661, 2021.
6. I. R. Reid, "Targeting Sclerostin in Postmenopausal Osteoporosis: Focus on Romosozumab and Blosozumab," *Biodrugs*, vol. 31, no. 4, pp. 289–297, 2017.
7. M. Qi, L. Zhang, Y. Ma, et al., "Autophagy Maintains the Function of Bone Marrow Mesenchymal Stem Cells to Prevent Estrogen Deficiency-Induced Osteoporosis," *Theranostics*, vol. 7, no. 18, pp. 4498–4516, 2017.
8. W. Chen, X. Chen, A. C. Chen, et al., "Melatonin restores the osteoporosis-impaired osteogenic potential of bone marrow mesenchymal stem cells by preserving SIRT1-mediated intracellular antioxidant properties," Free Radical Biology and Medicine, vol. 146, pp. 92–106, 2020.
9. Y. Ma, M. Qi, Y. An, et al., "Autophagy controls mesenchymal stem cell properties and senescence during bone aging," Aging Cell, vol. 17, no. 1, Article ID e12709, 2018.
10. J. Kiernan, J. E. Davies, and W. L. Stanford, "Concise Review: Musculoskeletal Stem Cells to Treat Age-Related Osteoporosis," Stem Cells Transl Med, vol. 6, no. 10, pp. 1930–1939, 2017.
11. X. Wang, T. Liang, J. Qiu, et al., "Melatonin Reverses the Loss of Stemness Induced by TNF-alpha in Human Bone Marrow Mesenchymal Stem Cells through Upregulation of YAP Expression," *Stem Cells Int*, vol. 2019, Article ID 6568394, 2019.
12. Y. Liu, L. Wang, T. Kikuiri, et al., "Mesenchymal stem cell-based tissue regeneration is governed by recipient T lymphocytes via IFN-gamma and TNF-alpha," Nature Medicine, vol. 17, no. 12, pp. 1594–1601, 2011.
13. H. Wei, Y. Xu, Y. Wang, et al., "Identification of Fibroblast Activation Protein as an Osteogenic Suppressor and Anti-osteoporosis Drug Target," *Cell Rep*, vol. 33, no. 2, Article ID 108252, 2020.
14. A. Huynh, D. M. Arnold, J. G. Kelton, et al., "Characterization of platelet factor 4 amino acids that bind pathogenic antibodies in heparin-induced thrombocytopenia," Journal of Thrombosis and Haemostasis, vol. 17, no. 2, pp. 389–399, 2019.
15. F. Pucci, S. Rickelt, A. P. Newton, et al., "PF4 Promotes Platelet Production and Lung Cancer Growth," Cell Rep, vol. 17, no. 7, pp. 1764–1772, 2016.

16. S. Struyf, M. D. Burdick, E. Peeters, et al., "Platelet factor-4 variant chemokine CXCL4L1 inhibits melanoma and lung carcinoma growth and metastasis by preventing angiogenesis," Cancer Research, vol. 67, no. 12, pp. 5940–5948, 2007.
17. I. Nazy, R. Clare, P. Staibano, et al., "Cellular immune responses to platelet factor 4 and heparin complexes in patients with heparin-induced thrombocytopenia," Journal of Thrombosis and Haemostasis, vol. 16, no. 7, pp. 1402–1412, 2018.
18. C. De Luca, A. M. Colangelo, L. Alberghina, and M. Papa, "Neuro-Immune Hemostasis: Homeostasis and Diseases in the Central Nervous System," *Frontiers in Cellular Neuroscience*, vol. 12, Article ID 459, 2018.
19. A. J. Affandi, S. C. Silva-Cardoso, S. Garcia, et al., "CXCL4 is a novel inducer of human Th17 cells and correlates with IL-17 and IL-22 in psoriatic arthritis," European Journal of Immunology, vol. 48, no. 3, pp. 522–531, 2018.
20. A. Dubrac, C. Quemener, E. Lacazette, et al., "Functional divergence between 2 chemokines is conferred by single amino acid change," *Blood*, vol. 116, no. 22, pp. 4703–4711, 2010.
21. I. Bruns, D. Lucas, S. Pinho, et al., "Megakaryocytes regulate hematopoietic stem cell quiescence through CXCL4 secretion," Nature Medicine, vol. 20, no. 11, pp. 1315–1320, 2014.
22. S. Kulkarni, and S. P. Jackson, "Platelet factor XIII and calpain negatively regulate integrin alphaIIbbeta3 adhesive function and thrombus growth," Journal of Biological Chemistry, vol. 279, no. 29, pp. 30697–30706, 2004.
23. V. K. Lishko, V. P. Yakubenko, T. P. Ugarova, and N. P. Podolnikova, "Leukocyte integrin Mac-1 (CD11b/CD18, alphaMbeta2, CR3) acts as a functional receptor for platelet factor 4," Journal of Biological Chemistry, vol. 293, no. 18, pp. 6869–6882, 2018.
24. S. Aidoudi, K. Bujakowska, N. Kieffer, and A. Bikfalvi, "The CXC-chemokine CXCL4 interacts with integrins implicated in angiogenesis," PloS One, vol. 3, no. 7, Article ID e2657, 2008.
25. C. Y. Su, J. Q. Li, L. L. Zhang, et al., "The Biological Functions and Clinical Applications of Integrins in Cancers," Frontiers in Pharmacology, vol. 11, Article ID 579068, 2020.
26. P. Moreno-Layseca, J. Icha, H. Hamidi, and J. Ivaska, "Integrin trafficking in cells and tissues," Nature Cell Biology, vol. 21, no. 2, pp. 122–132, 2019.
27. S. Saleem, J. Li, S. P. Yee, et al., "beta1 integrin/FAK/ERK signalling pathway is essential for human fetal islet cell differentiation and survival," Journal of Pathology, vol. 219, no. 2, pp. 182–192, 2009.
28. J. Chen, T. Chen, Y. Zhu, et al., "circPTN sponges miR-145-5p/miR-330-5p to promote proliferation and stemness in glioma," Journal of Experimental and Clinical Cancer Research, vol. 38, no. 1, Article ID 398, 2019.
29. A. Flores-Perez, D. G. Rincon, E. Ruiz-Garcia, et al., "Angiogenesis Analysis by In Vitro Coculture Assays in Transwell Chambers in Ovarian Cancer," Methods in Molecular Biology, vol. 1699, pp. 179–186, 2018.
30. P. Pozarowski, and Z. Darzynkiewicz, "Analysis of cell cycle by flow cytometry," Methods in Molecular Biology, vol. 281, pp. 301–311, 2004.

31. M. Fenelon, M. Etchebarne, R. Siadous, et al., "Assessment of fresh and preserved amniotic membrane for guided bone regeneration in mice," Journal Of Biomedical Materials Research Part A, vol. 108, no. 10, pp. 2044–2056, 2020.
32. D. Huang, H. Hu, L. Chang, et al., "Chinese medicine Bazi Bushen capsule improves lipid metabolism in ovariectomized female ApoE-/- mice," Ann Palliat Med, vol. 9, no. 3, pp. 1073–1083, 2020.
33. J. A. Hampel, J. Rinkinen, J. R. Peterson, et al., "Early Development of the Mouse Morphome," Journal of Craniofacial Surgery, vol. 27, no. 3, pp. 621–626, 2016.
34. T. Yamaji, K. Ando, S. Wolf, P. Augat, and L. Claes, "The effect of micromovement on callus formation," Journal of Orthopaedic Science, vol. 6, no. 6, pp. 571–575, 2001.
35. Y. Jiang, W. Luo, B. Wang, et al., "Resveratrol promotes osteogenesis via activating SIRT1/FoxO1 pathway in osteoporosis mice," Life Sciences, vol. 246, Article ID 117422, 2020.
36. L. Cui, S. Xu, D. Ma, et al., "The role of integrin-alpha5 in the proliferation and odontogenic differentiation of human dental pulp stem cells," Journal of Endodontics, vol. 40, no. 2, pp. 235–240, 2014.
37. L. Zhang, G. Jiao, S. Ren, et al., "Exosomes from bone marrow mesenchymal stem cells enhance fracture healing through the promotion of osteogenesis and angiogenesis in a rat model of nonunion," Stem Cell Research & Therapy, vol. 11, no. 1, Article ID 38, 2020.
38. A. Sinclair, L. Park, M. Shah, et al., "CXCR2 and CXCL4 regulate survival and self-renewal of hematopoietic stem/progenitor cells," *Blood*, vol. 128, no. 3, pp. 371–383, 2016.
39. H. Liu, W. Li, Y. Liu, X. Zhang, and Y. Zhou, "Co-administration of aspirin and allogeneic adipose-derived stromal cells attenuates bone loss in ovariectomized rats through the anti-inflammatory and chemotactic abilities of aspirin," Stem Cell Research & Therapy, vol. 6, Article ID 200, 2015.
40. L. S. Coimbra, J. P. Steffens, M. N. Muscara, C. Rossa, Jr., and L. C. Spolidorio, "Antiplatelet drugs reduce the immunoinflammatory response in a rat model of periodontal disease," Journal of Periodontal Research, vol. 49, no. 6, pp. 729–735, 2014.
41. L. S. Coimbra, J. P. Steffens, C. Rossa, Jr., D. T. Graves, and L. C. Spolidorio, "Clopidogrel enhances periodontal repair in rats through decreased inflammation," Journal of Clinical Periodontology, vol. 41, no. 3, pp. 295–302, 2014.
42. J. J. Chen, Y. Gao, Q. Tian, Y. M. Liang, and L. Yang, "Platelet factor 4 protects bone marrow mesenchymal stem cells from acute radiation injury," British Journal of Radiology, vol. 87, no. 1040, Article ID 20140184, 2014.
43. S. Viale-Bouroncle, M. Gosau, and C. Morsczeck, "Laminin regulates the osteogenic differentiation of dental follicle cells via integrin-alpha2/-beta1 and the activation of the FAK/ERK signaling pathway," Cell and Tissue Research, vol. 357, no. 1, pp. 345–354, 2014.
44. S. V. Chandran, M. Vairamani, and N. Selvamurugan, "Osteostimulatory effect of biocomposite scaffold containing phytomolecule diosmin by Integrin/FAK/ERK signaling pathway in mouse mesenchymal stem cells," *Scientific Reports*, vol. 9, no. 1, Article ID 11900, 2019.

45. Y. J. Chen, Y. Y. Wei, H. T. Chen, et al., "Osteopontin increases migration and MMP-9 up-regulation via alphavbeta3 integrin, FAK, ERK, and NF-kappaB-dependent pathway in human chondrosarcoma cells," Journal of Cellular Physiology, vol. 221, no. 1, pp. 98–108, 2009.
46. C. Zou, Q. Luo, J. Qin, et al., "Osteopontin promotes mesenchymal stem cell migration and lessens cell stiffness via integrin beta1, FAK, and ERK pathways," Cell Biochemistry and Biophysics, vol. 65, no. 3, pp. 455–462, 2013.

Figures

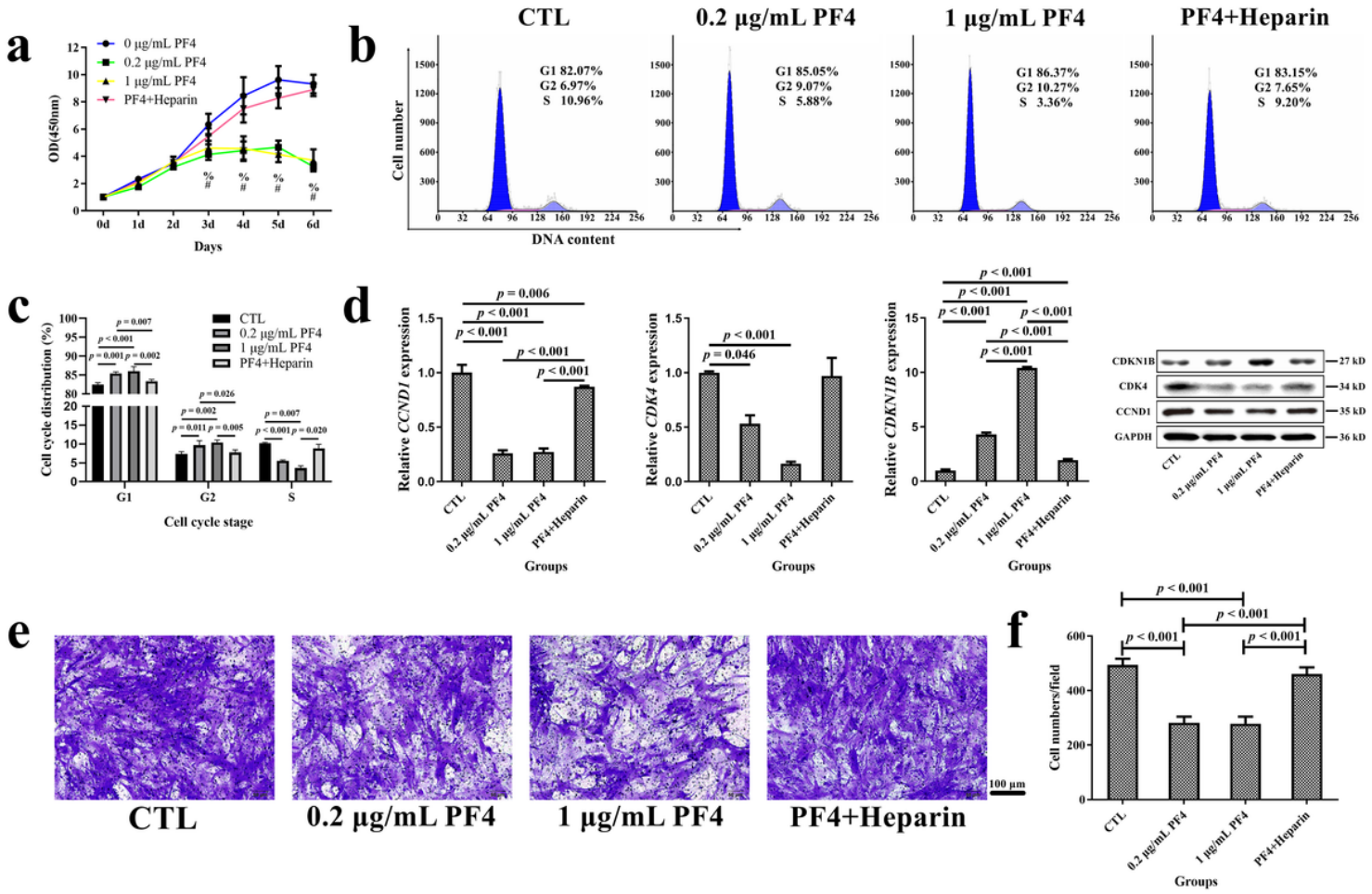

Figure 1

PF4 suppressed the cell proliferation and migration of BMMSCs *in vitro*. (a) The cellular proliferation rate of BMMSCs was evaluated using a CCK8 assay in four groups. (b) Representative FCM images on cell cycle of BMMSCs in the four groups. (c) The cell cycle distribution on BMMSCs was detected by FCM in the four groups. (d) The relative gene and protein expression levels related to the cell cycle was assessed by *q*PCR and WB in each of the four groups. (e) Representative images of BMMSC migration in each of the four groups (stained with a crystal violet solution). Scale bar = 100 μm. (f) The BMMSC migration ability was analyzed by transwell assay. N = 6 samples per group. Data are expressed as the mean ± SD of experiments undertaken in triplicate. #$p < 0.05$ compared with 0 μg/mL PF4; %$p < 0.05$ compared with

PF4+Heparin. PF4, platelet factor 4; BMMSCs, bone marrow mesenchymal stem cells; FCM, flow cytometry; *q*PCR, quantitative real-time polymerase chain reaction; WB, Western blotting; CCND1, cyclin D1; CDK4, cyclin dependent kinase 4; CDKN1B, cyclin dependent kinase inhibitor 1B; GAPDH, glyceraldehyde-3-phosphate dehydrogenase.

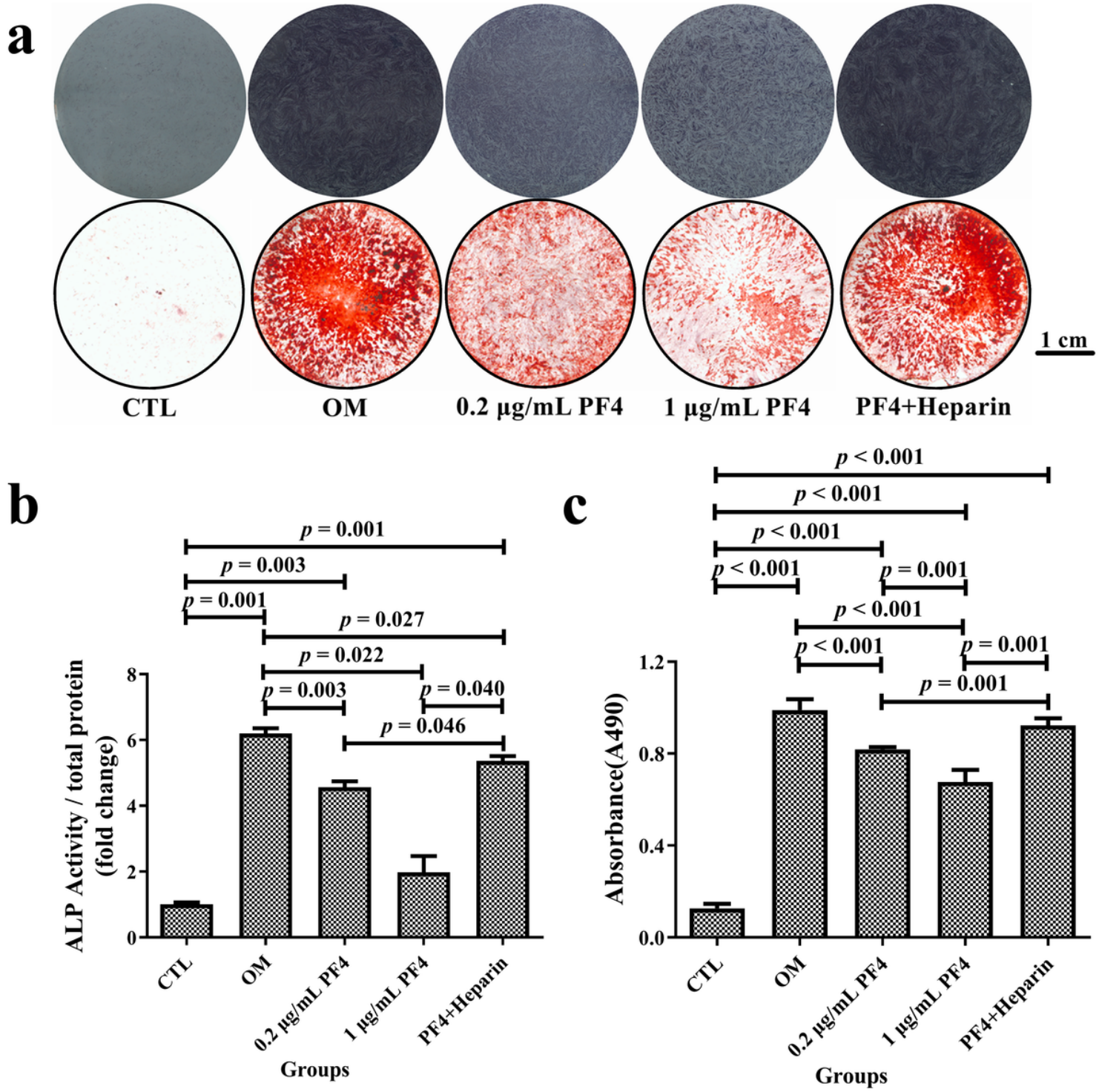

Figure 2

PF4 attenuated the osteogenic differentiation ability of BMMSCs *in vitro*. **a** Representative image of ALP and ARS staining of BMMSCs in each of the five groups. Scale bar = 1 cm. The ALP quantitative analysis (**b**) and ARS semiquantitative analysis (**c**) of the BMMSCs was evaluated in each of the five groups. N = 6 samples per group. Data are expressed as the mean ± SD of experiments undertaken in triplicate. PF4, platelet factor 4; BMMSCs, bone marrow mesenchymal stem cells; ALP, alkaline phosphatase; ARS, alizarin red S; OM: osteogenic medium.

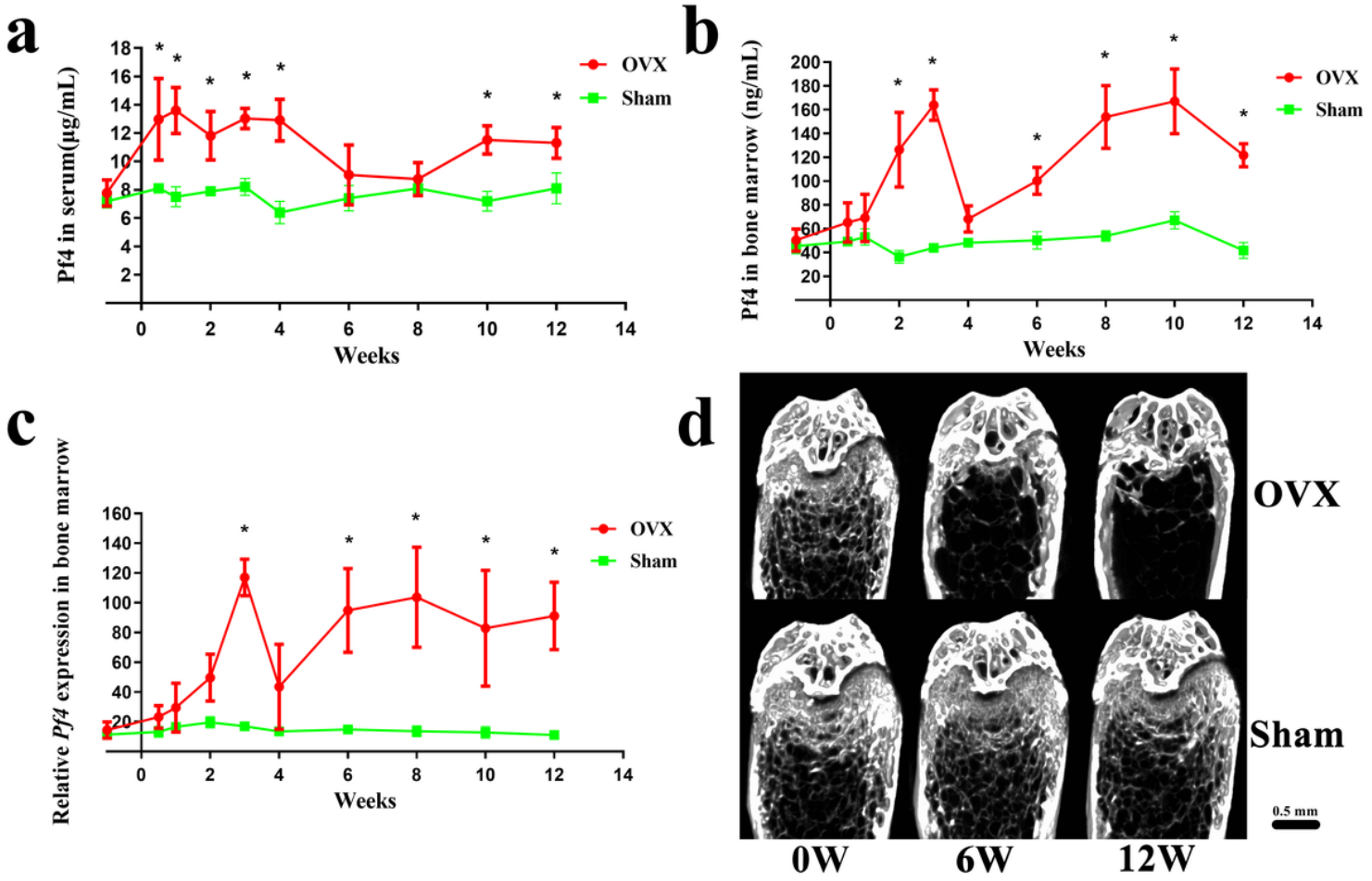

Figure 3

The level of Pf4 in the serum and BM were generally increased in OVX mice. The variation tendencyof Pf4 concentrations in the serum (**a**) and BM (**b**) in OVX and Sham mice (the samples were obtained every two weeks until 12 weeks, the baseline were obtained 1 week before OVX surgery). In general, the levels of Pf4 in serum and BM were increased in OVX mice compared with those of Sham group. **c** The variation tendency of relative *Pf4* expression in the BM of OVX and Sham mice (the samples were obtained every two weeks until 12 weeks, the baseline were obtained 1 week before OVX surgery). The variation tendency of the relative expression of *Pf4* in the BM was analogous to the Pf4 concentration in the BM and exhibited a more robust change. **d** Representative images of the femurs on coronal planes reconstructed by microCT in OVX and Sham mice at 0, 6, and 12 weeks after OVX surgery. Femur of OVX mice exhibited a severe bone loss at 6 and 12 weeks compared with those of Sham mice. Scale bar = 0.5 mm. N = 6

mice per group. Data are expressed as the mean ± SD. *$p < 0.05$ compared with Sham group. BM, bone marrow; OVX, ovariectomy; Pf4/*Pf4*, platelet factor 4.

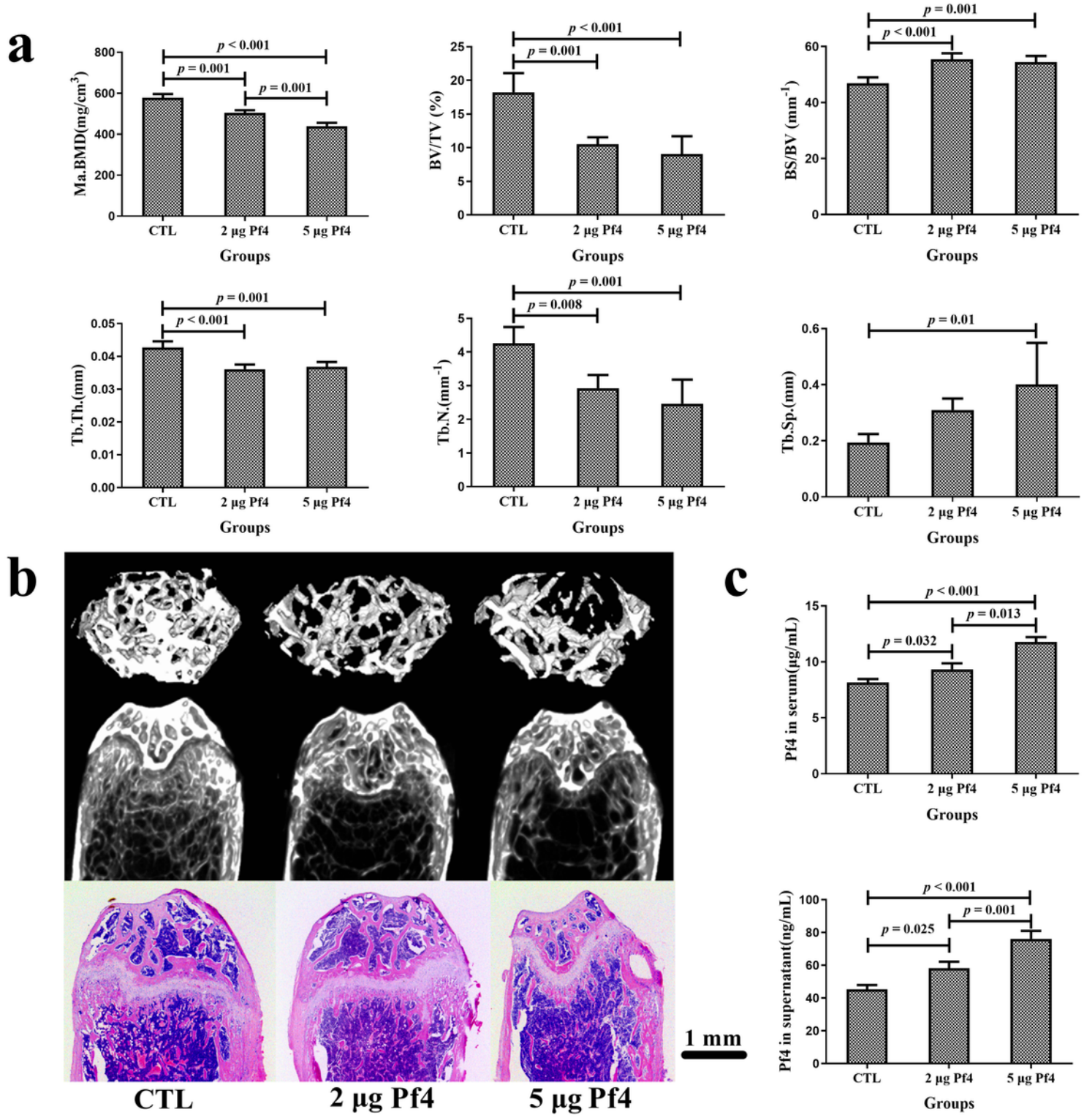

Figure 4

Pf4 supplementation triggered bone loss in the mice at 8 weeks. **a** BMD and bone histomorphometry of the femurs in mice at 8 weeks after an injection of different doses of Pf4 in three groups. In short, the

BMD and bone microarchitecture of the femur decreased along with the increasing dose of Pf4 injection. **b** Representative images of the femurs reconstructed by microCT (horizontal and coronal planes) and slicing stained by H&E (coronal plane) at 8 weeks after Pf4 injection in three groups. Scale bar = 1 mm. **c** The level of Pf4 in the serum and BM at 8 weeks following Pf4 injection in three groups. N = 10 mice per group. Data are expressed as the mean ± SD. Pf4, platelet factor 4; Ma.BMD, bone mineral density of bone marrow; BV/TV, bone volume/total volume; BS/BV, bone surface area/bone volume; Tb.Th, trabecular thickness; Tb.N, trabecular number; Tb.Sp, trabecular separation; H&E, hematoxylin and eosin.

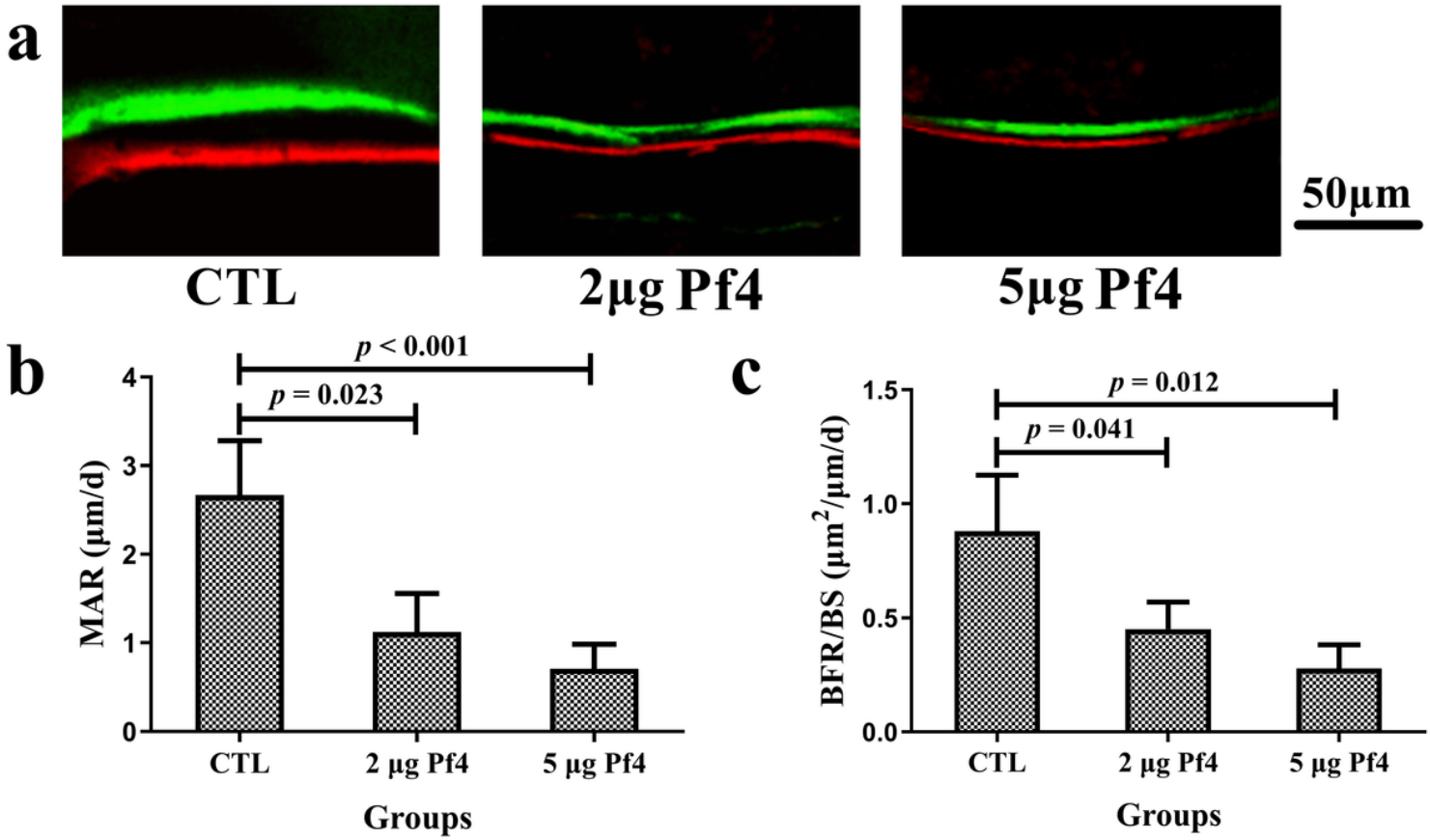

Figure 5

Supplementation of Pf4 decreased the bone formation rate in mice at 8 weeks. **a** Representative fluorescence images from undecalcified bone slicing of the femur after double labeling with calcein (green fluorescence band) and alizarin-3-methyliminodiacetic acid (red fluorescence band). The green and red fluorescence bands respectively represented new bone formation area at 10th and 3rd day prior to euthanasia and the interval of two fluorescence bands represented the bone formation rate between 7 days. Scale bar = 50 μm. The increased area and interval of two fluorescence bands represented the better ability on bone formation. MAR (**b**) and BFR/BS (**c**) were evaluated through the fluorescence images from undecalcified bone slicing of the femur using Bioquant software. N = 10 mice per group. Data are expressed as the mean ± SD. Pf4, platelet factor 4; MAR, mineral apposition rate; BFR/BS, bone formation rate/bone surface.

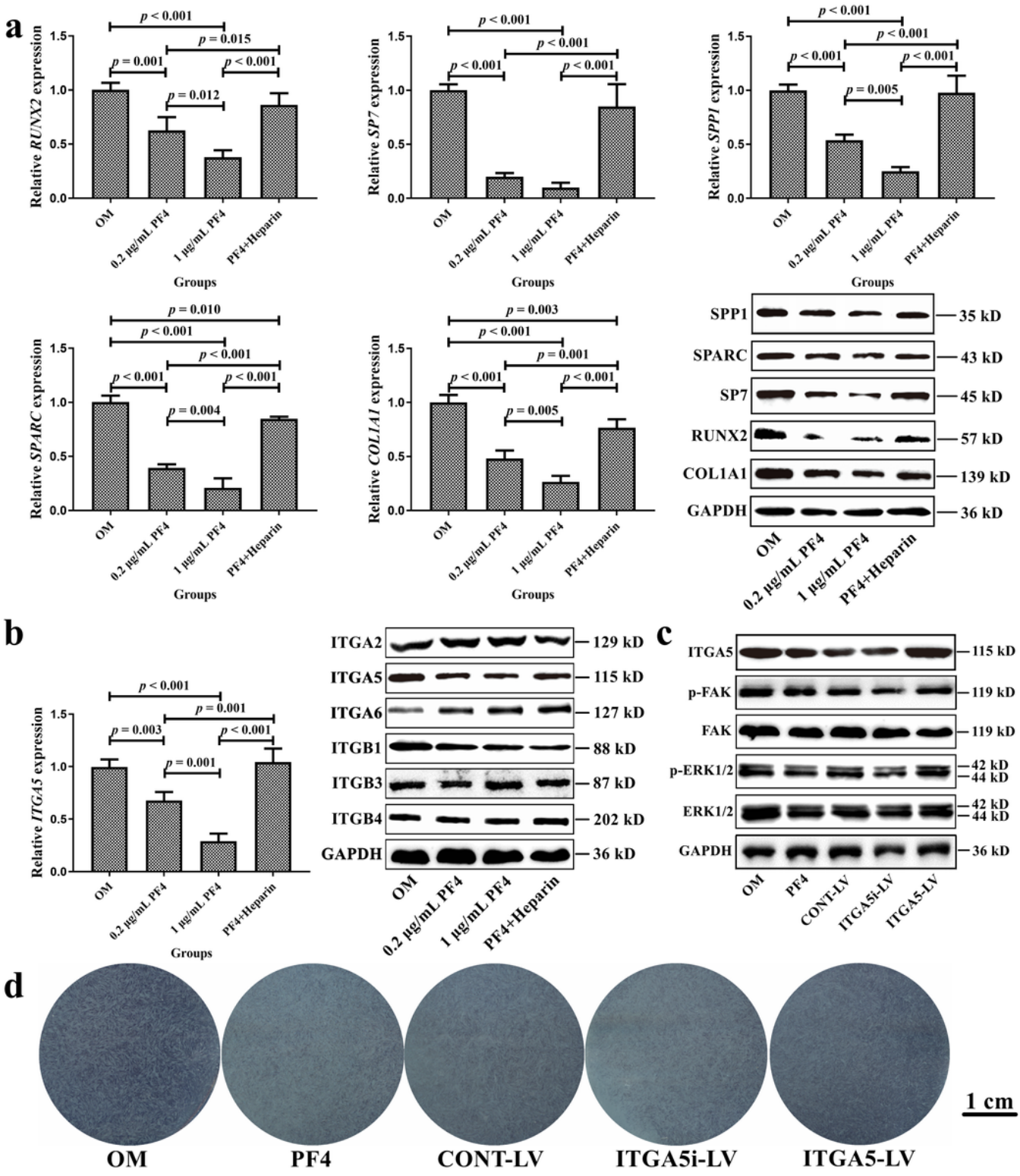

Figure 6

PF4 down-regulated osteogenic gene expression by inhibiting the ITGA5-FAK-ERK pathway. **a** The relative gene and protein expression levels related to osteogenesis were assessed by *q*PCR and WB in OM, 0.2 μg/mL PF4, 1 μg/mL PF4, and PF4+Heparin groups. **b** The relative *ITGA5* expression and protein expression levels of 6 typical integrin subunits were assessed by *q*PCR and WB in OM, 0.2 μg/mL PF4, 1 μg/mL PF4, and PF4+Heparin groups. **c** WB on ITGA5, p-FAK, FAK, p-ERK1/2, and ERK1/2 were evaluated

among OM, PF4, CONT-LV, ITGA5i-LV, and ITGA5-LV groups. **d** Representative images of ALP staining of BMMSCs among OM, PF4, CONT-LV, ITGA5i-LV, and ITGA5-LV groups. Scale bar = 1 cm. N = 6 samples per group. Data are expressed as the mean ± SD of the experiments undertaken in triplicate. PF4, platelet factor 4; RUNX2, RUNX family transcription factor 2; SP7, Sp7 transcription factor; SPP1, secreted phosphoprotein 1; SPARC, secreted protein acidic and cysteine rich; COL1A1, collagen type I alpha 1 chain; ITGA2/5/6, integrin α2/5/6; ITGB1/3/4, integrin β1/3/4; *q*PCR, quantitative real-time polymerase chain reaction; BMMSCs, bone marrow mesenchymal stem cells; WB, Western blotting; p-FAK, phosphorylated focal adhesion kinase; p-ERK, phosphorylated extracellular regulated protein kinases; GAPDH, glyceraldehyde-3-phosphate dehydrogenase; OM: osteogenic medium; CONT-LV: control lentivirus; ITGA5i-LV: ITGA5 interfering lentivirus; ITGA5-LV: ITGA5 overexpression lentivirus.

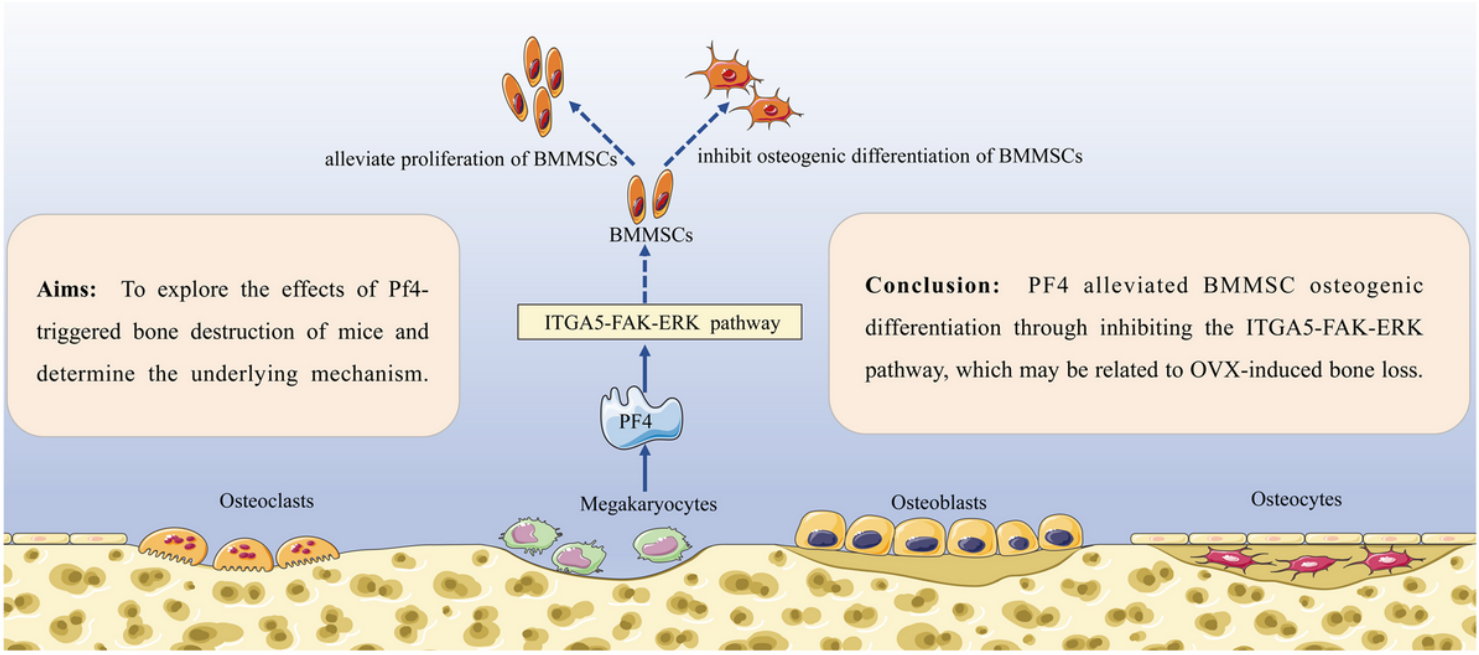

Figure 7

Overview of the proposed pathways for PF4-induced bone loss.

Supplementary Files

This is a list of supplementary files associated with this preprint. Click to download.

- Supplementarymaterials.docx